Available online at www.sciencedirect.com
ScienceDirect
Journal of Photochemistry and Photobiology A: Chemistry 188 (2007) 226–234
Journal of Photochemistry and Photobiology A:Chemistry
www.elsevier.com/locate/jphotochem

Preparation and characterization of doped metal-supported TiO_2-layers

Corinna Graf [a,*], Renate Ohser-Wiedemann [b], Günter Kreisel [a]

[a] *Friedrich-Schiller-University Jena, Department of Technical and Environmental Chemistry, Lessingstraße 12, 07743 Jena, Germany*
[b] *TU Bergakademie Freiberg, Institute of Materials Science, Gustav-Zeuner-Strasse 5, 09599 Freiberg, Germany*

Received 11 September 2006; received in revised form 20 November 2006; accepted 11 December 2006
Available online 16 December 2006

Abstract

Defined doping of metal-supported TiO_2-layers is possible by using cerium or gadolinium complex-precursors in anodic spark deposition processes. Thereby CeO_2 und $Gd_2Ti_2O_7$ species are formed in TiO_2-layers and the concentration of anatase increases. Studies using XRD, REM, TGA, DTA und HPLC have been carried out and characteristics of the surface were defined. The doping of TiO_2 using cerium and gadolinium results in a decreasing BET surface area. The band-gap determination of cerium doped samples offers a blue-shift. These results are reflected in studies of photocatalytic activity using reaction of methanol conversion. Gadolinium doped titanium dioxide showed better photocatalytic activity than cerium doped sample possibly because of the stability of Gd^{3+}-ions.

Keywords: Heterogeneous photocatalysis; TiO_2; Doping; Cerium; Gadolinium; Rare earth

1. Introduction

In recent years, photo-induced reactions on semiconductors attract widespread interest, particularly in regard to photocatalysis on TiO_2 [1]. Use of sunlight for photocatalytic purposes is the aim of many studies, which can be achieved by bathochromic shift into visible light.

Doping with lanthanids is a method to shift the maximum of absorption as well as enhance the photocatalytic activity. Simultaneous a shift of anatase-to-rutile-ratio to pure anatase phases is reached [2]. In addition doping procedures of TiO_2 with nitrogen [3], silver-ions [4], gold-ions [5], palladium and copper [6] or zinc-ions [7] were studied.

The sol–gel-route is widely used to prepare doped and undoped TiO_2, but in the most cases, powders with differences in particle sizes are obtained. There are few alternative procedures to prepare fixed and metal-supported TiO_2 coatings. It is well-known [8] that metal oxides are formed on passivated metals using anodic spark deposition. This treatment was advanced in our department [9]. We are able to coat substrates of different materials, versatile forms and surface characteristics using the SOLECTRO®-process. In this process a titanium substrate in contact with the anode is dipped into an electrolyte bath, containing the titanium-precursor titanyl acetylacetonate, which is formed during the electrolyte preparation. Impressing a voltage greater than 100 V on the substrate, a layer of TiO_2 is formed in several minutes. We know that the formed TiO_2 is deposited on the substrate from the electrolyte. The obtained layers are well characterized and their photocatalytic activity is documented [10]. In former studies, pure TiO_2-layers were prepared. The first aim of this work is to dope TiO_2-layers with cerium and gadolinium, and the second is to study the effects of morphology, composition of the layers, surface properties, and the extent of the band-gap and photocatalytic activity. Furthermore all samples were annealed at 400–950 °C to study the influence of the heating temperature on the composition of samples, average particle size and photocatalytic activity.

2. Experimental

Pure titanium substrates were used (1.2 mm thickness, dimension 1 cm × 1 cm) as anode. A special electrolyte for coating with pure TiO_2 was prepared. To achieve doped samples via the SOLECTRO®-process a compound of cerium

* Corresponding author. Tel. +49 3641 948435; fax: +49 3641 948402.
E-mail addresses: corinna.graf@uni-jena.de (C. Graf), wiedemann@ww.tu-freiberg.de (R. Ohser-Wiedemann), guenter.kreisel@uni-jena.de (G. Kreisel).

1010-6030/$ – see front matter © 2007 Elsevier B.V. All rights reserved.
doi:10.1016/j.jphotochem.2006.12.019

Table 1
Composition of doped and undoped electrolytes for using in SOLECTRO®-process

Compound	Concentration (mol/l)
Ethylendiammintetraacidic acid disodiumsalt, p.a., VWR	0.1
Ammonia 25%, p.a., VWR	0.007
Ammonium acetate, p.a., Fluka	0.013
Acetylacetone, p.a., VWR	0.5
2-Propanol, p.a., Roth	0.65
Tetraethylorthotitanat, p.a., VWR	0.05
Only for preparation of doped electrolytes: cerium(III) acetylacetonate hydrate, p.a., Aldrich	2.5×10^{-3}
Gadolinium(III) acetylacetonate hydrate, p.a., Aldrich	2.5×10^{-3}

Table 2
Annealing temperatures and concentration of dopand in electrolyte for preparation of TiO_2 layers

Samples	Dopand	Concentration of dopand in electrolyte (mmol/l)	Annealing temperature (°C)
TiO_2	–	–	400, 550, 750, 950
TiO_2/4 wt.% Ce	Cerium	2.5	400, 550, 750, 950
TiO_2/4 wt.% Gd	Gadolinium	2.5	400, 550, 750, 950

or gadolinium was added into electrolyte during preparation procedure. The composition of undoped and doped electrolytes is given in Table 1.

A voltage of 180 V and a current of 10 A (maximum) were impressed by a special control unit. The voltage reached in steps of 10 V/s the setpoint at 180 V and was hold for 180 s. Afterwards all samples were washed with deionised water and dried on air overnight. Then samples were annealed at different temperatures. Table 2 contains sample marking and the annealing temperatures. Heating at 400 °C is necessary for all samples, because organic compounds, which incorporate into TiO_2 in SOLECTRO®-process, were decomposed. At this temperature the transformation from anatase to rutile was not initiated. For additional experiments TiO_2 layers were annealed at temperatures up to 950 °C and the furnace was heated with 3 °C/min. This temperature was hold for 3 h. These experiments were done to investigate formation of cerium and gadolinium compounds in the layers and to study the behaviour of annealed layers in methanol conversion.

The layer thickness is measured by means of the analyzer Surfix® (PHYNIXGmbH&Co.KG) based on eddy current technique. An average over 10 measurements was used for evaluation. Afterwards TiO_2-layers were mechanically striped, sampled and weighted (Fig. 2).

The X-ray diffraction (XRD) spectra of the coatings were recorded with a Seifert-FPM URD6 powder diffractometer using Cu Kα radiation and standard Bragg-Brentano diffraction geometry. The measurements were done in the angle range of 20–80° 2θ, with steps of 0.05° 2θ, and times of 20 s at each step. A monochromator was used in the secondary beam path. The phase analysis was realized by program REFLEX (Seifert FPM) using the PDF-database. The quantitative phase analyses were carried out by Rietveld-method (program BGMN, Seifert FPM). The volume fraction of every single phase and the particle size were determined.

The image of scanning electron microscope (SEM) was mapped with secondary and back scattered electrons (BSE) using 20 kV. The chemical composition of the samples was analyzed by SEM using energy disperse X-ray analysis.

To analyze BET-surface area all samples were realized using volumetric sorption automat Autosorb-1 (Quantachrome). The results were evaluated using Software Autosorb 1, and determination of pore size and specific pore volume were analyzed according to Barret–Joyner–Halenda (BJH).

Measurements of UV–vis diffuse reflectance spectroscopy were done using an integrating sphere named Cary 5000 UV–vis-NIR spectrophotometer (Varian). Appraisal of results occurred by program Scan.

Samples of quantitative analysis were mechanically stripped, powders were weighted, and 10 ml of aqua regia, nitric acid and concentrated hydrochloric acid were successively added. After addition the samples were softly evaporated till nearly dryness. Then the next acid was added. At the end of heating, suspensions were added with deionised water, transferred in a volumetric flask and fulfilled with deionised water and the deposits sedimented for 48 h. The above solution was analyzed using ICP-MS. Residues were filtered, dried at 120 °C, decomposed using potassium hydrogen sulfate [11] and solved in distilled water. All samples were analysed by unit SpectroFlame (Spectro). These measurements occurred to validate the results, which are obtained using XRD.

For photocatalytic activity determination 25 mg 2,4-dinitrophenylhydrazine (DNPH, recrystallized in acetonitrile) were solved in 5 ml acetonitrile (HPLC-grade). Ten milliliter of hydrochloric acid (1 mol/l) were added, stirred and afterwards filtered. A quartz-vessel (layer thickness $d = 1$ cm) was filled with 1 ml of solution (1 vol.% methanol in deionised water, methanol HPLC-grade, VWR; deionised water, Millipore). Following a TiO_2 layer (1 cm × 1 cm) was irradiated in this solution for 7 min. A xenon arc lamp XBO 450 W (Mueller Elektronik GmbH) was used for radiation. Intensity of light were 1.8 mW/cm^2 in the UVA-range and 150 mW/cm^2 in the Vis-range of 400–800 nm on position of the sample (using measuring instruments UVM-CP of firm A.C. Peschl and NIST Traceable PHOTOMETER Model IL1400A, International Light). At the end of irradiation the solution was transferred by pipette into HPLC-vial, and 50 μl of DNPH-solution was added. Vials were shaked at room temperature at 600 RPM using IKA-VIBRAX-VXR for 1.5 h. Then the samples were analyzed using HPLC pump model M480, autosampler Gina 50 and diodenarray detector UVD 340S (all Gynkotek), column was a Knaur Eurospher 100-C18 with 4.00 mm inside diameter and 25 cm length, eluent consists of acetonitrile (70 vol.%, HPLC-grade) and deionised water (30 vol.%, Millipore). The flow was 1800 μl/min, and 20 μl were injected. The wavelength of 360 nm was used for measurements.

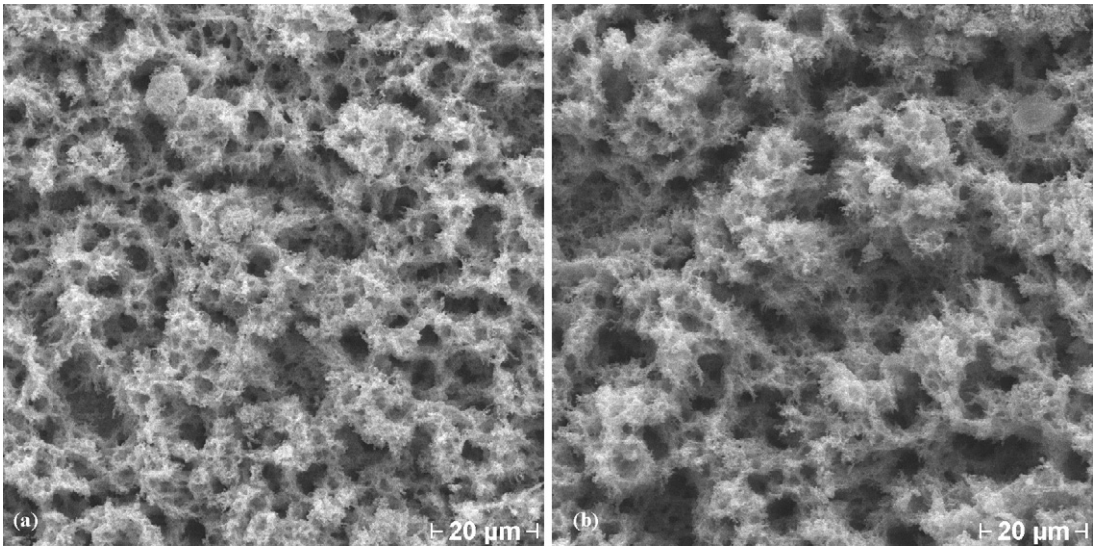

Fig. 1. SEM-images, which show morphology of (a) pure SOLECTRO®-TiO_2 and (b) cerium doped SOLECTRO®-TiO_2.

3. Results

3.1. Layer characteristics—morphology, layer thickness and BET-surface area

The pure SOLECTRO® TiO_2-layers consist of a filigree and coral-like structure. As it shown in Fig. 1 addition of dopands has no significant influence of surface morphology. If the layers were prepared under the same conditions then the morphology is not influenced by the dopand elements and their concentrations.

After annealing the color of surface has changed. If samples were doped using cerium, then layers turned yellow after annealing. The doping using gadolinium results in white layers.

Average results of layer thickness measurement are shown in Fig. 2.

The addition of cerium and gadolinium organic compounds into the electrolyte (2.5 mmol/l) tends to thicker layers with higher masses, although all layers are prepared under the same conditions. Reasons for this phenomenon of thicker layers are unknown. Measurements of conductivity, kinematic viscosity, density and pH-value of the used electrolytes indicated that these characteristics could be excluded as a reason.

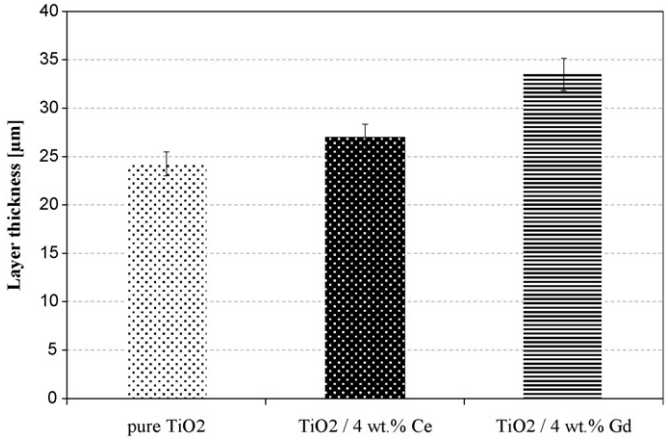

Fig. 2. Layer thickness of pure and doped TiO_2-samples. The coated area was 10 cm^2 and finally normed to 1 m^2. S.D. was 1.34%.

The results of BET-surface area measurements are given in Table 3 and the BET adsorption isotherms are shown in Fig. 3. In contrast to pure TiO_2-layers (show Fig. 3a) doped samples get a lower BET-surface area, e.g. which is shown in Fig. 3b. The analysis shows that all samples consist of mesopores, but their volume decreases with the addition of dopands. It is generally agreed, that decreasing of BET-surface areas cause a lower photocatalytic activity.

3.2. Chemical composition

Different concentrations of dopands were realized in the electrolytes. The chemical analysis of cerium and gadolinium content in the layers shows that the increase of dopand concentration in electrolyte is correlated with an increase of the dopand concentration in the layer (Fig. 4).

It is noticeable, that adding 1 mmol/l of dopand compound effects deposition of nearly 2 wt.% dopand in layer. These results were also obtained for gadolinium layers, too. We believe that the formation of doped layers takes place in the same way like deposition of pure TiO_2 layers. According to titanium a lanthanid precursor is formed during the electrolyte preparation as we described in the introduction. We believe that in the SOLECTRO®-process the lanthanids and titanium were simultaneously deposited on the titanium substrate. Therefore the concentration of lanthanids in the layer only depends on the given lanthanide concentration in the electrolyte.

All samples were analysed by X-ray diffraction. As it is shown in Fig. 5a–c, titanium dioxide still exists in its modifications as anatase and rutile in all samples, in pure layers as well as in doped samples. The layer thickness of tested samples was lower than the penetration depth of an electron beam so the response of titanium from the support is evident in diagrams.

Crystalline oxides of cerium and gadolinium were only detected at higher annealing temperatures. CeO_2 was formed in

Table 3
Surface properties of pure and doped TiO_2-layers

Sample	BET-surface area (m^2/g)	BJH-pore diameter (Å)	Specific pore volume (cm^3/g)	Monolayer capacity (mg_{N_2}/g_{sample})
Pure TiO_2	55	38	0.16	15.9
TiO_2/4 wt.% Ce	43	38	0.14	12.4
TiO_2/4 wt.% Gd	35	38	0.12	10.1

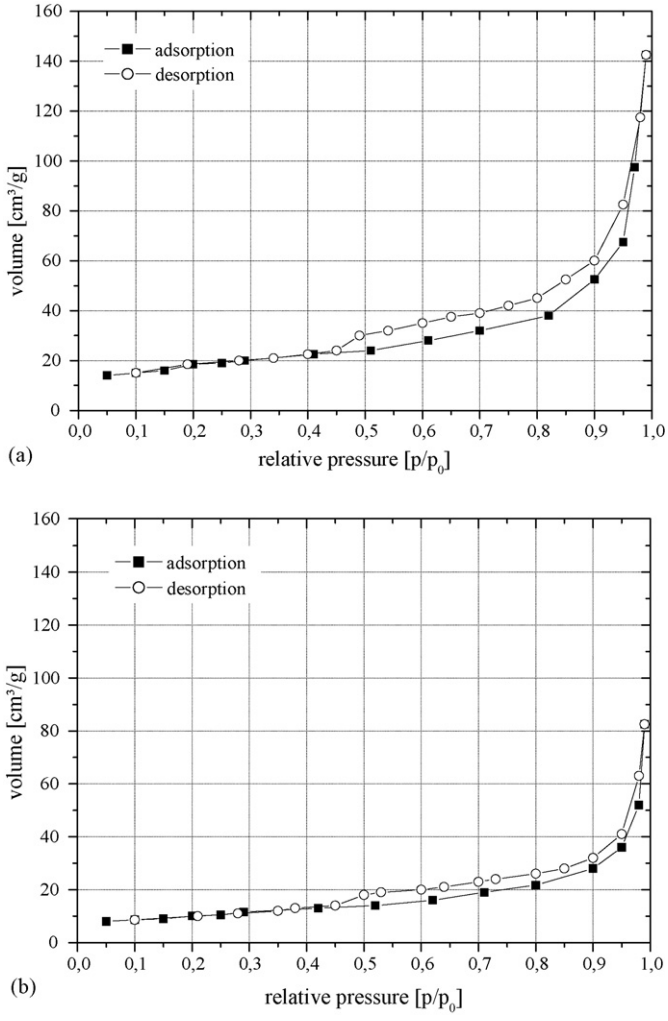

Fig. 3. BET adsorption isotherms of (a) pure TiO_2 and (b) gadolinium doped TiO_2, for example.

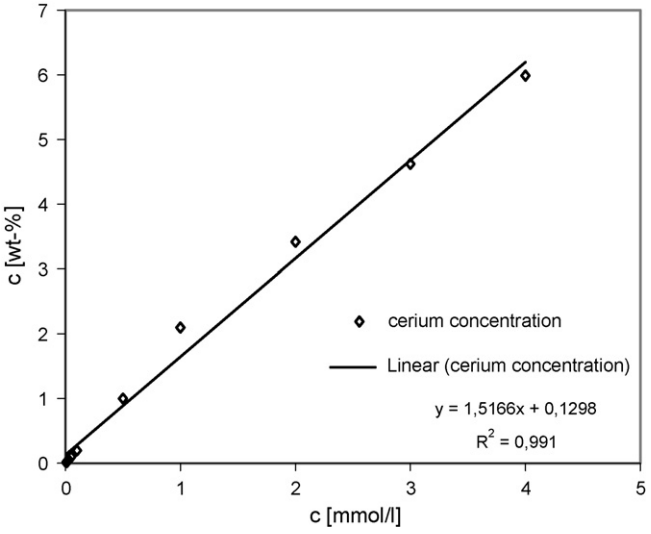

Fig. 4. Correlation of dopand concentration (here: cerium, i.e.) in electrolyte (*x*-axis) to dopand concentration in layer (*y*-axis). These results are transferable to gadolinium doped TiO_2-layers.

cerium-doped samples at 750 °C and samples offered a yellow color. $Gd_2Ti_2O_7$ was formed in gadolinium-doped TiO_2-layers at 950 °C. These samples are white.

Cerium- and gadolinium-doped samples, which were annealed at 400 and 550 °C, were decomposed using potassium bisulfate and analyzed using ICP-MS. It was noticed, that in this samples the same concentration of dopands exists as in samples, which were annealed at 950 °C. By contrast, no oxide phases of cerium- or gadolinium-compounds (annealed at 400 and 550 °C) were detected using XRD.

It is possible, that oxides of cerium and gadolinium are amorphous at 400 and 550 °C. The results of quantitative phase analysis are shown in Fig. 6. The incorporation of cerium or gadolinium compounds causes the shift of anatase to rutile ratio to higher anatase fraction. In comparison with standard SOLECTRO® TiO_2-layers (anatase:rutile = 20%:80%) was the ratio of anatase of doped and annealed (at 400 °C) samples redoubled (47%:53%). It is remarkable that crystalline phases of cerium and gadolinium compounds were not detected in doped samples, but a shift of anatase to rutile ratio could be achieved. Content of anatase decreases, if annealing temperature increases, and at temperatures above 900 °C only rutile phase is detectable, accompanied by oxides of cerium and gadolinium. In addition oxidation of the titanium substrate takes place. A higher photocatalytic activity was expected for samples with higher anatase content.

Fig. 7 shows the average particle size of both phases. The average particle size increases with increasing annealing temperature as expected. In this case the conversion of anatase to rutile is nearly completed at 750 °C. Here the content of anatase was so low, that the particle size could not be exactly detect. The particle size of anatase and rutile are nearly the same at 400 and 550 °C, but the particle size of pure TiO_2 increases.

By cerium and gadolinium doped TiO_2-layers the anatase phase was detected after annealing at 750 °C. The particle size of anatase is approximately the same as the particle size of rutile. In conclusion it is possible, that cerium and gadolinium inhibit phase transformation of anatase to rutile because of their presence and their atom radii. Rare earth elements and TiO_2 form Ti–O–rare earth element bonds, and these bonds stabilize the anatase phase [12,13]. These results are in accordance with the

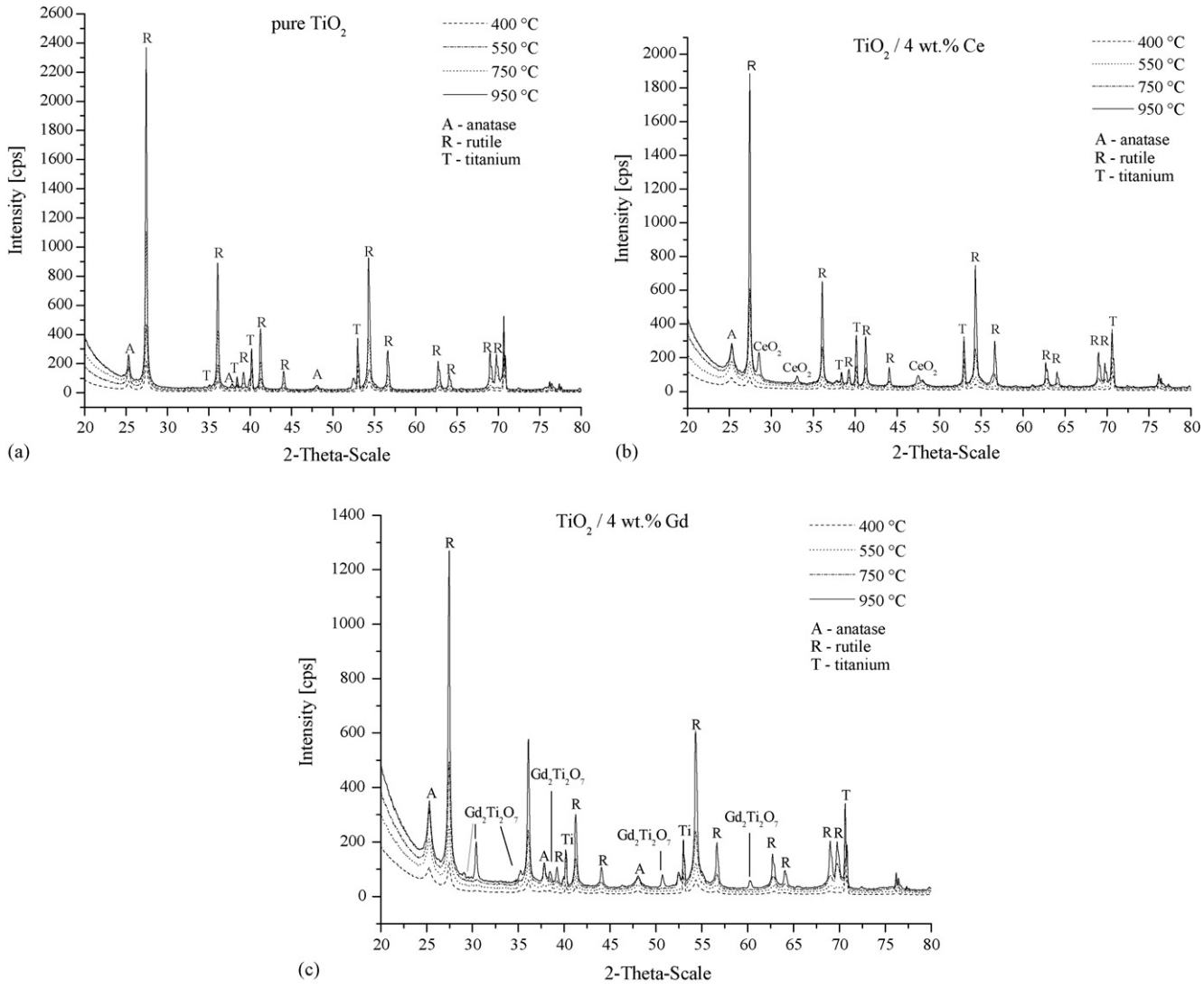

Fig. 5. X-ray diffraction (a) of pure TiO_2-layer on a titanium support. This TiO_2-layer was defined as standard. (b) X-ray diffraction of gadolinium-doped TiO_2-layer (4 wt.%) and (c) of cerium-doped TiO_2-layer (4 wt.%).

results of Xu et al. [2] and Jiang et al. [14]. Theoretical analysis showed that the particle size plays an important role in photocatalysis of TiO_2. A stochastic model postulates an increase of quantum yield, if particle size increases from 3 to 21 nm [15]. According to this an advanced photocatalysis of TiO_2 layers can be expected for particle sizes at 20 nm.

The XRD-measurements could not explicitly verify the incorporation of cerium or gadolinium in the anatase or rutile lattice. Precise determination of lattice constants will be a part of future investigations to solve this problem. Table 4 summarizes the results obtained by X-ray diffraction method. Concentrations of dopands in layers were validated using ICP-MS measurements.

3.3. Band gap and photocatalytic activity

One factor, which influences photocatalytic activity of semiconductors, is the width of the band gap. The energy used for the transfer of electron from the valence band to the conduction band can be calculated (is known). The band gap of all samples was determined using UV–vis-spectroscopy. Diffuse reflectance spectra are shown in Fig. 8. Following the results of analysis obtained for all samples are given in Table 5. But it is notable that this method of determining band gap using integrated spheres is not very exact. The obtained spectra were graphically analyzed by attaching a tangent on the graph's slope and another tangent is attached on the linear component of the graph between 200 and 325 nm. The intersection point of both tangents indicates the band gap in nanometers. It is comprehensible that adjusting tangents is not very exact. In present works we want to determine the band gap once more using Mott–Schottky-plot.

The band gap of pure anatase phase is noted at 3.23 eV, and of pure rutile phase is found at 3.02 eV. In this work the band gap of pure TiO_2 layer (annealed at 400 °C) was found at 3.36 eV. Furthermore if layers were annealed at 950 °C the band gap decreases. The reason for this behavior is most likely the phase composition of the layer (100% rutile). The same effect is observable in cerium and gadolinium doped samples. In contrast TiO_2/Ce-samples possess a higher band gap than pure TiO_2

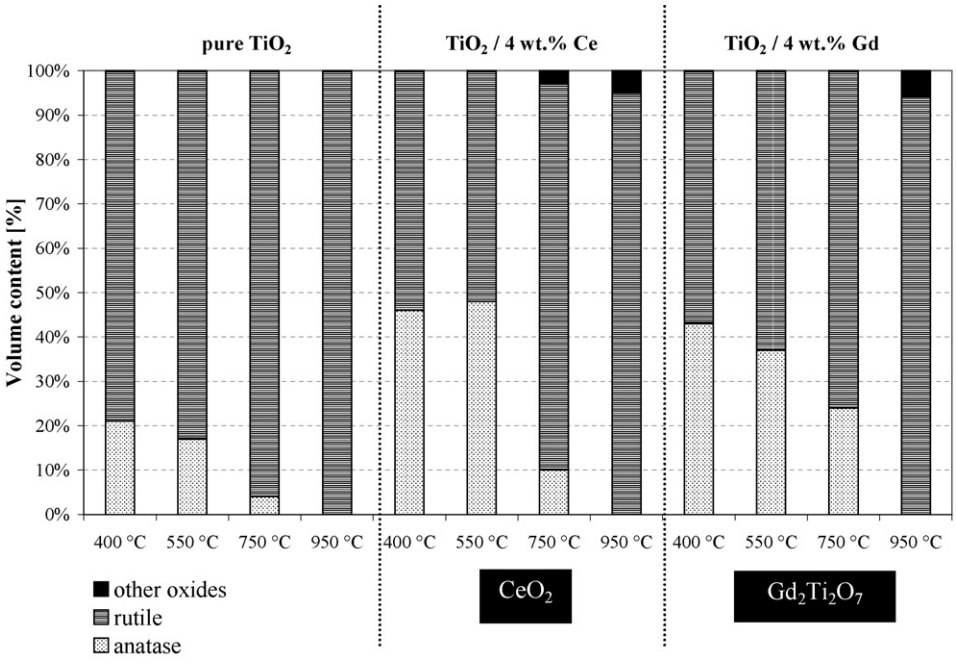

Fig. 6. Content of anatase, rutile and other oxides and mixed oxides using different annealing temperatures.

layers, but gadolinium doped samples possess of lower band gap. It is known, that pure $Gd_2Ti_2O_7$ has a band gap at 3.5 eV [16] or 354 nm, and CeO_2 has it at 2.9 eV [17] or 427.5 nm. Reddy and Khan [18] determined a band gap of a mixed oxide CeO_2–TiO_2 in the range of 2.88 eV. Hence the change of band gap cannot be only a result of CeO_2 or $Gd_2Ti_2O_7$ formation, but also the formation of pure rutile phase encroaches upon these circumstances.

In former works of Kaessbohrer [19] a method for photocatalysts screening based on their activity was developed. This method is based on an abstraction of α-hydrogen atom because of the presence of hydroxyl radicals, shown in the following equation:

$$OH^{\bullet} + CH_3OH \rightarrow H_2O + {}^{\bullet}CH_2OH$$

The hydroxymethyl radical is formed because of the illumination of the TiO_2 photocatalyst and it reacts with solved oxygen of the solution to formaldehyde. This is described in equation:

$${}^{\bullet}CH_2OH + O_2 \rightarrow {}^{\bullet}O_2CH_2OH \rightarrow HCHO + HO_2{}^{\bullet}$$

According to Asmus et al. [20] methanol is attracted by OH-radicals at the α-hydrogen atom for 93%. For 7% methanol

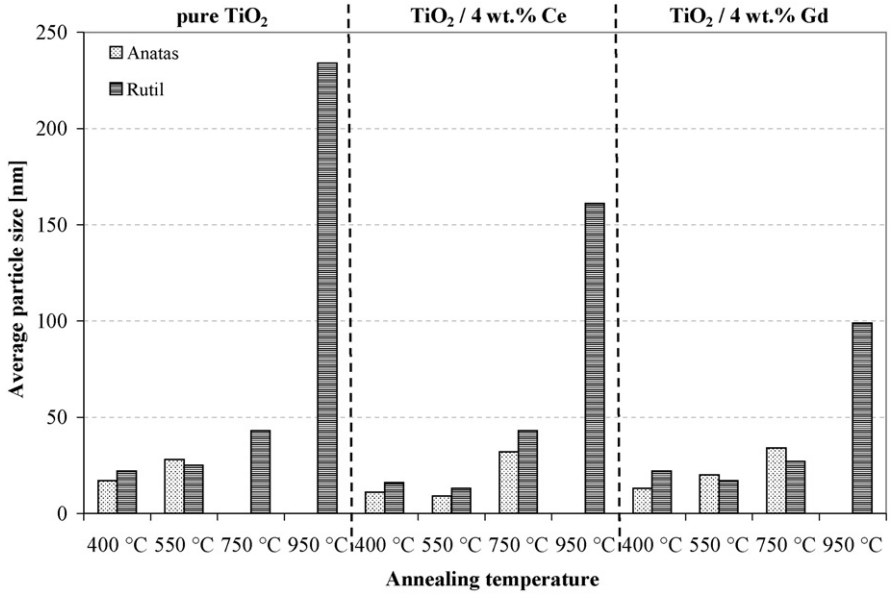

Fig. 7. Determination of average particle size of metal-supported pure and doped TiO_2-layers.

Table 4
Summary of all results

Parameter	Sample name		
	Pure TiO_2	TiO_2/4 wt.% Ce	TiO_2/4 wt.% Gd
Dopand concentration in electrolyte (mol/l)	–	2.5×10^{-3}	2.5×10^{-3}
Dopand concentration in layer (wt.%)	–	4	4
Average layer thickness (μm)	24	27	33.5
Average mass of layer (g/m^2)	16	22	27

Temperature (°C)	Sample name					
	Pure TiO_2		TiO_2/4 wt.% Ce		TiO_2/4 wt.% Gd	
	Anatase	Rutile	Anatase	Rutile	Anatase	Rutile
Phase analysis (vol.%)						
400	21	79	46	54	43	57
550	17	83	48	52	37	63
750	4	96	10	87[a]	24	76
950	0	100	0	95[b]	0	94[c]
Average particle size (nm)						
400	17	22	11	16	13	22
550	28	25	9	13	20	17
750	–	43	32	43	34	27
950	–	234	–	161	–	99

[a] 3 vol.% CeO_2.
[b] 5 vol.% CeO_2.
[c] 6% $Gd_2Ti_2O_7$.

is attracted at OH-hydrogen. There are no other results for SOLECTRO®-TiO_2-layers, so this ratio was underlain, too. Formed formaldehyde was obtained by 2,4-dinitrophenylhydrazine (DNPH) derivatisation to formaldehyde-2,4-dinitrophenylhydrazone (FDNPH). Both substances, DNPH as well as FDNPH, are detectable at 360 nm using HPLC.

Experiment was done for pure and cerium and gadolinium doped TiO_2-layers. Fig. 9 shows concentrations of formed OH-radicals depending on annealing temperature.

The obtained results showed, that doping using cerium and gadolinium results in a lower formation of hydroxyl radicals compared to pure TiO_2 samples. Thus photocatalytic activity decreases because of doping, but cerium-doped and gadolinium-doped samples differ in their photocatalytic formation of OH-radicals. And annealing temperature has a bearing on generation of OH-radicals. It is shown in results that samples, which were annealed at 400 °C, possess highest yield of OH-radicals. If annealing temperature increases or decreases, OH-radical generation decreases.

4. Discussion

Metal-supported pure and doped TiO_2 layers (doped with 4 wt.% cerium or gadolinium) were prepared using SOLECTRO®-process. Significant changes in layer characteristics, composition and photocatalytic activity were induced. The control of concentration of the dopand in the layer was achieved by changing its concentration in the electrolyte.

CeO_2-phases and $Gd_2Ti_2O_7$-phases are formed at 750 and 950 °C, and in comparison to pure TiO_2 layers the anatase to rutile ratio was shifted in cerium and gadolinium doped samples. The reason for the ratio shift could be found in phase transformation from anatase to rutile caused by lanthanids inhibition [2,12–14]. Furthermore lanthanids inhibit grow of crystallites, and in this manner the average particle size of anatase and rutile is still 35–40 nm at annealing temperatures of 750 °C. These results indicate that photocatalytic activity of doped samples could be better than activity of pure TiO_2. But using the method of methanol conversion it was shown, that doped samples generate

Table 5
Band gaps of pure and doped TiO_2-samples, which were annealed at different temperatures

Sample name	Annealing temperature (°C)	Band gap (nm) ± error (nm)	Band gap (eV) ± error (eV)
Pure TiO_2	400	369 ± 3	3.36 ± 0.03
	950	395 ± 4	3.14 ± 0.04
TiO_2/4 wt.% Ce	400	351 ± 4	3.53 ± 0.04
	950	388 ± 6	3.20 ± 0.06
TiO_2/4 wt.% Gd	400	388 ± 4	3.20 ± 0.04
	950	393 ± 5	3.15 ± 0.05

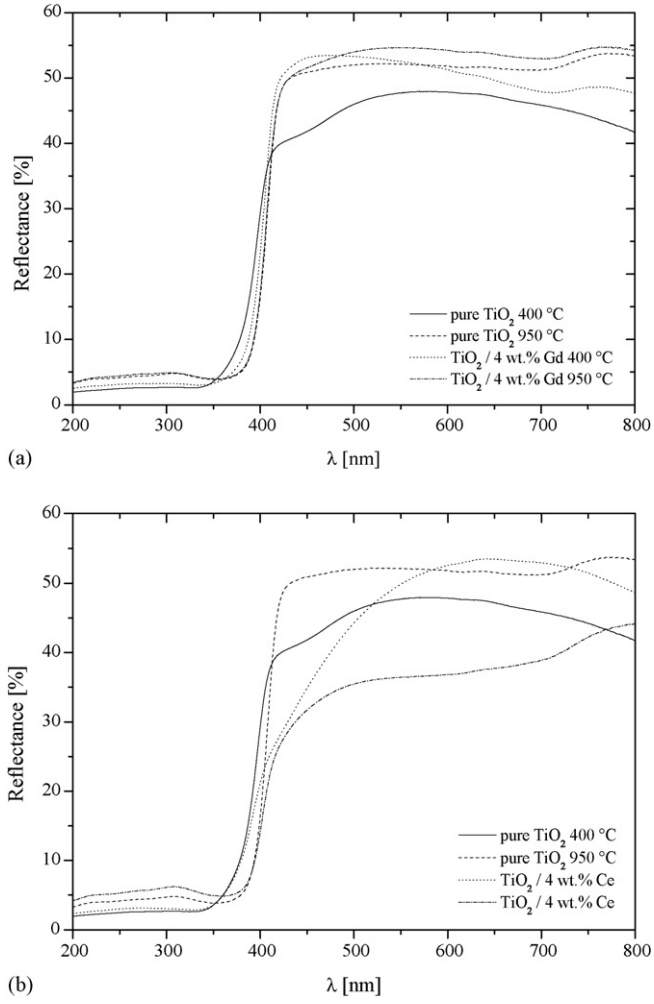

Fig. 8. Results of diffuse reflectance spectroscopy for pure and doped TiO_2-layers.

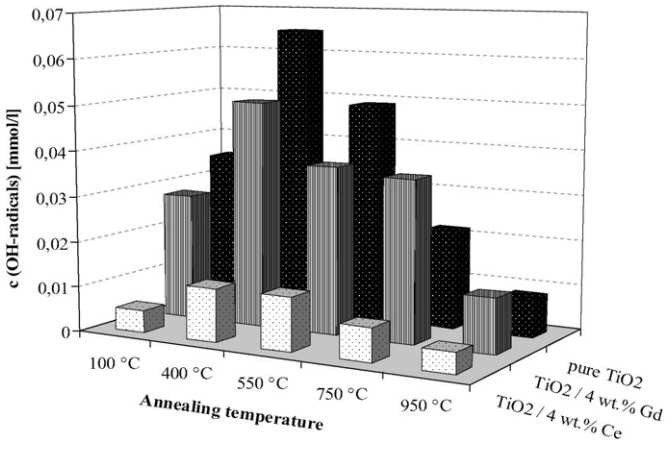

Fig. 9. Results of methanol conversion by irradiation (7 min) using xenon arc lamp XBO 450 W (UVA = 1.8 mW/cm^2, Vis = 150 mW/cm^2) for 7 min, and following derivatization.

fewer hydroxyl radicals than pure TiO_2 layers. The assignable cause may be that due to the decrease in BET surface of the doped samples less active centres are available.

Doping of TiO_2 using cerium results in a higher band gap compared to pure TiO_2. A less band gap and a bathochromic shift of the absorption maximum were reached by using gadolinium doping. But how it was shown, the bathochromic shift does not result in a better photocatalytic activity. Perhaps this is a consequence of large reduction of BET-surface area of gadolinium-doped TiO_2 layers. Reduction of BET-surface area of cerium-doped samples is not so significant. Photocatalytic activity is proved to be a mixture of different influences, i.e. width of band gap, BET-surface area and particle size.

Samples, which were annealed at 950 °C, consist of rutile phase and a phase of the dopand compound. In all samples they posses the lowest yield of hydroxyl radicals. On the one hand, this result is due to dimension of formed particles (>200 nm). On the other hand, adsorbed hydroxyl groups and water molecules are desorbed at high temperatures. In this case, an artificial hydrophobicity is induced. Thus, attached water cannot find any point of contact on the surface. Consequently formed electrons and holes cannot react while they form hydroxyl radicals using solved oxygen. It is possible that recombination processes of electron–hole pairs are preferred.

It is noticeable that gadolinium doped TiO_2 layers generate more hydroxyl radicals than cerium doped samples. It is possible, that the kind of formed compound, in which cerium or gadolinium is embedded, plays an important role. Cerium builds an independent oxide, CeO_2. But gadolinium is combined with titanium, and they form the mixed oxide $Gd_2Ti_2O_7$. In this mixed oxide hetero-cations were embedded using valences smaller than Ti^{4+}, Gd^{3+} (called n-doping). Thus the dopand acts as an acceptor, which catches photo generated electrons. Additionally Gd^{3+} posses a half filled electron configuration (f^7) and is very stable. If Gd^{3+} gets an electron, so this electron configuration is destroyed. But trapped electrons can be transferred to adsorbed oxygen species on the surface, and in this way a stable electron configuration is recovered. This procedure is the propulsion of formation of the hydroxyl radicals and effects an effective separation of electron-hole-pairs [21].

It was shown in subsequent experiments that used dopand concentration of 4 wt.% was very high. Photocatalytic activity is improved in comparison to pure TiO_2 layers using lower concentrated samples (0.01–0.1 wt.%). It is possible that lower concentrated samples achieve a better separation of electron–hole pairs, because there is an optimum of dopand concentration in the layer. Preparation of samples with 4 wt.% dopand was especially done to analyse modified layers. Works of the topic "photocatalysis with lower concentrated samples" will be finished soon.

Achieved results show, that all facts to influence photocatalytic activity interdigitate each other. And so it is necessary to consider not only an increase of the anatase content, but also other properties like the kind of formed dopand compound, hydrophobicity, particle size, BET-surface and other layer properties.

Acknowledgement

Authors would like to thank Dr. Schreiber, TU Bergakademie Freiberg, for his assistance with XRD measurements.

References

[1] H. Kisch, W. Macyk, Nachrichten aus der Chemie 50 (2002) 1078.
[2] A.-W. Xu, Y. Gao, H.-Q. Liu, J. Catal. 207 (2002) 151.
[3] S.L. Chen, X.G. Diao, Y.J. Zhang, T.M. Wang, Ra. Met. Mat. Eng. 33 (2004) 36.
[4] P. Falaras, I.M. Arabatzis, T. Stergiopoulos, M.C. Bernard, Int. J. Photoen. 5 (2003) 123.
[5] F.B. Li, X.Z. Li, X.Y. Li, Acta Chim. Sinica 59 (2003) 1072.
[6] J. Arana, J.M. Dona-Rodriguez, J.A.H. Melian, E.T. Rendon, O.G. Diaz, J. Photochem. Photobiol. A 174 (2005) 7.
[7] G.G. Liu, X.Z. Zhang, Y.J. Xu, X.S. Niu, L.Q. Zheng, X.J. Di, Chemosphere 59 (2005) 1367.
[8] N.P. Sluginov, Zh. Ross fiz, Khim. Obsh. 15 (1883) 232.
[9] I. Hennig, J. Käßbohrer, G. Kreisel, U. Bayer, U. Weinzierl, Deutsches Patent DE 198 41 650 A1 (2006).
[10] S. Meyer, Dissertation, 2003, Jena.
[11] G. Jander, Lehrbuch der Analytischen und Präparativen Anorganischen Chemie, S. Hirzel Verlag, Stuttgart, 1995, p. 532.
[12] M.S.P. Francisco, V.R. Mastelaro, Chem. Mater. 14 (2002) 2514.
[13] J. Lin, J.C. Yu, J. Photochem. Photobiol. A 116 (1998) 63.
[14] H.-Q. Jiang, P. Wang, D.-D. Lu, L.-Y. Wu, H.-Z. Xiann, Chin. J. Inorg. Chem. 22 (2006) 73.
[15] M. Grela, A.J. Colussi, J. Phys. Chem. 100 (1996) 18214.
[16] R. Abe, M. Higasi, K. Sayama, Y. Abe, H. Sugihara, J. Phys. Chem. B 110 (2006) 2219.
[17] G.R. Bamwenda, H. Arakawa, J. Mol. Catal. A 161 (2000) 105–113.
[18] B.M. Reddy, A. Khan, Asian Catal. Surv. 9 (2005) 155–171.
[19] J. Käßbohrer, Diplomarbeit, 1997, Jena.
[20] K.-D. Asmus, H. Möckel, A. Henglein, J. Phys. Chem. 10 (1973) 1218.
[21] O. Carp, C.L. Huisman, A. Reller, Prog. Sol. Chem. 32 (2004) 33.